



NLR TP 97006

## **Impact damage and failure mechanisms in structure relevant composite specimens**

J.F.M. Wiggeraad and L.C. Ubels

DOCUMENT CONTROL SHEET

	ORIGINATOR'S REF. NLR TP 97006 U		SECURITY CLASS. Unclassified																					
ORIGINATOR National Aerospace Laboratory NLR, Amsterdam, The Netherlands																								
TITLE Impact damage and failure mechanisms in structure relevant composite specimens																								
PRESENTED AT the Eleventh International Conference on Composite Materials (ICCM-11), God Coast, Australia 14th - 18th July 1997																								
AUTHORS J.F.M. Wiggendaad and L.C. Ubels		DATE 970106	pp    ref 14    5																					
DESCRIPTORS <table style="width: 100%; border: none;"> <tr> <td style="width: 33%;">Composite structures</td> <td style="width: 33%;">Impact damage</td> <td style="width: 33%;">Wing panels</td> </tr> <tr> <td>Compression tests</td> <td>Laminates</td> <td></td> </tr> <tr> <td>Damage assessment</td> <td>Residual strength</td> <td></td> </tr> <tr> <td>Delaminating</td> <td>Specimen geometry</td> <td></td> </tr> <tr> <td>Failure models</td> <td>Stiffening</td> <td></td> </tr> <tr> <td>Graphite-epoxy composites</td> <td>Tolerance (mechanics)</td> <td></td> </tr> <tr> <td></td> <td>Ultrasonic flaw detection</td> <td></td> </tr> </table>				Composite structures	Impact damage	Wing panels	Compression tests	Laminates		Damage assessment	Residual strength		Delaminating	Specimen geometry		Failure models	Stiffening		Graphite-epoxy composites	Tolerance (mechanics)			Ultrasonic flaw detection	
Composite structures	Impact damage	Wing panels																						
Compression tests	Laminates																							
Damage assessment	Residual strength																							
Delaminating	Specimen geometry																							
Failure models	Stiffening																							
Graphite-epoxy composites	Tolerance (mechanics)																							
	Ultrasonic flaw detection																							
ABSTRACT Impact damage and failure mechanisms, representative of stiffened composite wing panels, were studied using small but structure relevant (SR) specimens. It was investigated how laminate stacking sequence influences the location within a laminate of the major delaminations that are generated by impact. Impact damages for six different lay-ups showed major delaminations predominantly at the ply interfaces where they were expected. Subsequently, the residual strength of the SR specimens was determined in compression. The major impact induced delaminations were also the delaminations that propagated under loading, driven by bending or buckling of the 0-degree plies. However, with increased loading, transverse shear of the delaminated sublaminates became the ultimate failure mechanism. Thus it was concluded that the residual strength of the SR specimens depends primarily on the reduced global stability of the damaged laminate, and less on the individual stability of the delaminated sublaminates. A failure criterion is needed, based on longitudinal compressive strain and transverse shear strain in 0-degree dominated ply stacks.																								
Keywords: Design, Impact, Damage Tolerance, Modelling and Testing.																								



## Contents

<b>Abstract</b>	5
<b>Keywords</b>	5
<b>1 Introduction</b>	5
<b>2 Panel design and SR specimen configuration</b>	6
<b>3 Experimental procedure</b>	7
<b>4 Results and discussion</b>	8
<b>5 Concluding remarks</b>	13
<b>6 Acknowledgements</b>	14
<b>7 References</b>	14
2 Tables	
8 Figures	

# IMPACT DAMAGE AND FAILURE MECHANISMS IN STRUCTURE RELEVANT COMPOSITE SPECIMENS

J.F.M. Wiggenraad and L.C. Ubels

*National Aerospace Laboratory NLR  
P.O. Box 153, 8300 AD Emmeloord, The Netherlands*

**ABSTRACT:** Impact damage and failure mechanisms, representative of stiffened composite wing panels, were studied using small but structure relevant (SR) specimens. It was investigated how laminate stacking sequence influences the location within a laminate of the major delaminations that are generated by impact. Impact damages for six different lay-ups showed major delaminations predominantly at the ply interfaces where they were expected. Subsequently, the residual strength of the SR specimens was determined in compression. The major impact induced delaminations were also the delaminations that propagated under loading, driven by bending or buckling of the 0-degree plies. However, with increased loading, transverse shear of the delaminated sublaminates became the ultimate failure mechanism. Thus it was concluded that the residual strength of the SR specimens depends primarily on the reduced global stability of the damaged laminate, and less on the individual stability of the delaminated sublaminates. A failure criterion is needed, based on longitudinal compressive strain and transverse shear strain in 0-degree dominated ply stacks.

**KEYWORDS:** Design, Impact, Damage Tolerance, Modelling and Testing

## 1. INTRODUCTION

The development of structural concepts for compression loaded, damage tolerant, stiffened composite wing panels requires an experimental investigation of the failure mechanisms that may occur. Insight into these mechanisms will lead to design guidelines for the structural configuration considered, and can be incorporated in design optimization procedures. One of the most critical states of damage to consider is the presence of one or more delaminations between the plies of a laminate, caused by low velocity impacts. Such delaminations tend to spread when the panel is loaded in compression, reducing the overall stability of the panel until ultimate failure occurs. (Delamination "spread" is defined as the quasi-static or dynamic propagation of a delamination under increased static loading, as opposed to delamination "growth" under fatigue loading).

The fabrication and testing of full scale stiffened panels is an expensive procedure, so for economic reasons most experiments are commonly performed on relatively simple specimens: plain laminates with corresponding material properties. When testing a laminate in the form of a small specimen supported by a frame, the damage resulting from the impact event as well as the residual compression strength may deviate considerably from the experimental values that are obtained when the laminate forms part of a larger structural configuration. Structural properties, such as the different dynamic response during impact and the presence of multiple load paths in a larger structure are thought to be responsible for the often superior damage tolerance observed when testing structures instead of small specimens.

At ICCM-9, a small Structure Relevant (SR) specimen was described [1], which is less expensive to make and test than a full scale panel. When combined with a support to simulate the stiffener [1-2], it maintains the essential design features of the panel configuration that is being investigated, see Fig. 1. The SR specimen was shown to be useful in providing insight

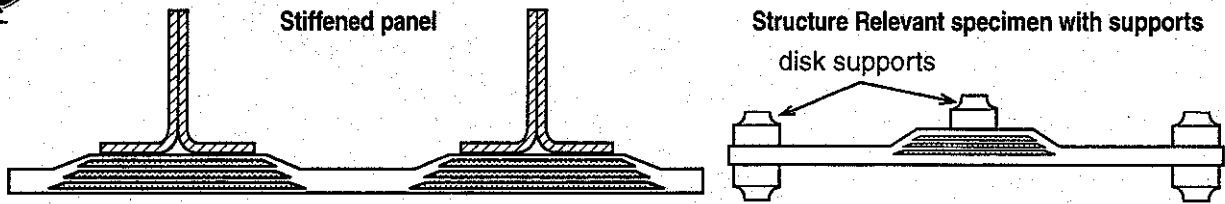


Fig. 1 Concept of Structure Relevant specimen

in delamination spread mechanisms. In this study, delaminations were provoked by the insertion of circular bronze foils. However, a proper evaluation of the damage tolerance of different design concepts requires that genuine damage is induced in the SR specimens by impact. This impact damage must correspond to the damage resulting from impacts on the stiffened panels that are represented by the SR specimens. At ICCM-10 a method was presented to apply structure relevant impact damage to SR specimens [3]. It was shown that the flexibility present in a larger structure can be approximated by selecting the proper support conditions for the SR specimen. It appeared that if the support conditions are such that the maximum deflection measured during impact at the impact site is approximately the same for stiffened panel and SR specimen, this will result in similar damage.

Based on the previous studies [1-3] it was believed that the failure mechanism related to the damage configuration considered, consists of the spread of a few preferred delaminations out of the multitude of delaminations and matrix cracks present in the impacted area, followed by sequential buckling of the delaminated sublaminates. When the overall stability of the panel reaches a critical value, ultimate failure occurs. As delamination spread occurs mainly in the lateral direction (perpendicular to the stiffeners) it is expected to start from delaminations with the widest span. The findings reported in [1-3] also revealed that the major impact induced delaminations are formed along certain preferred ply interfaces. Hence, it was postulated in [3] that by a deliberate positioning of these preferred interfaces deeper inside the laminate, thicker sublaminates will be formed by the impact. As thicker sublaminates have a higher resistance against buckling, delamination spread and ultimate failure are expected to be delayed when the specimen is loaded by increased compression.

In the present study the results are presented of a test programme, in which SR specimens with six different lay-ups were provided with impact damage and subsequently loaded in compression up to failure. The objectives of this programme were to investigate whether the major impact induced delaminations occur at the interfaces where they are expected, and to evaluate the validity of the postulated failure mechanism.

## 2. PANEL DESIGN AND SR SPECIMEN CONFIGURATION

The configuration of the SR specimens was based on a damage tolerant stiffened carbon/epoxy panel concept developed by Boeing [4], now applied in the V-22 Osprey wing. This concept

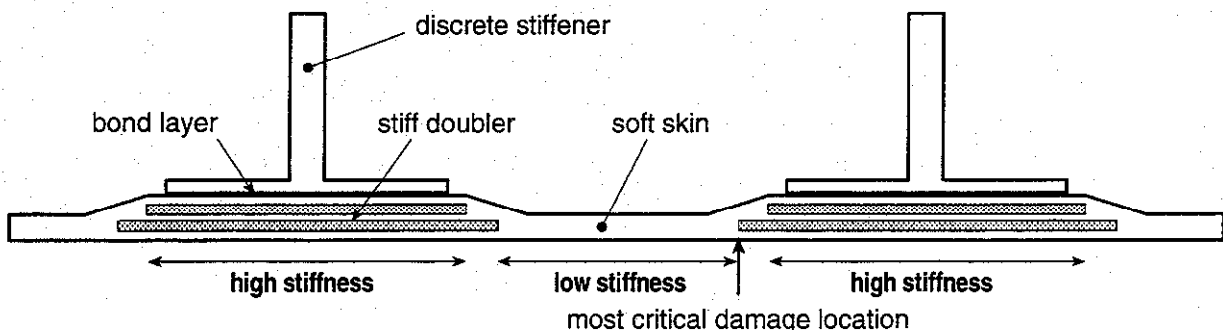


Fig. 2 Boeing's damage tolerant panel concept with soft skin, doublers and discrete stiffeners

comprises a soft (low axial stiffness) skin, doublers (extra plies added locally to the skin underneath the stiffeners) and discrete (pre-cured) stiffeners, see Fig. 2. A panel design with I-stiffeners was determined for an ultimate load level of 2000 N/mm, using the PANOPT optimization code for stiffened panels [5], see Fig. 3. One of the six SR specimen lay-ups was identical to the skin/doubler configuration of the panel design, while the other lay-ups were variations thereof. The lay-ups of the six different SR configurations are listed in table 1 and are shown in Fig. 4. In the present paper, results are discussed for five specimens of each lay-up.

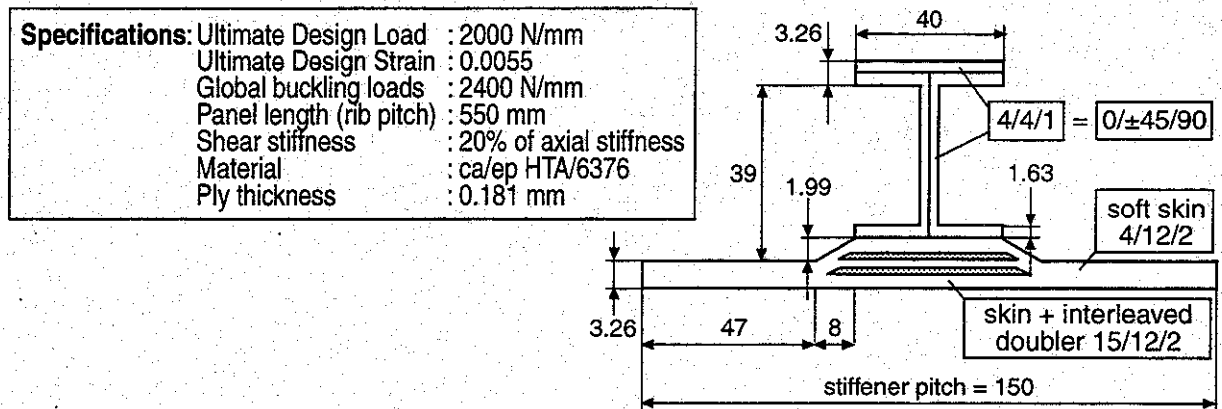


Fig. 3 Design specifications, geometry and lay-up (dimensions in mm)

Table 1: Laminate configurations

Configuration	Laminate stacking sequence (starting at flat side)
1	$(\pm 45)_2/0/[0_6]/90/(\pm 45)/0/[0_5]/0/(\mp 45)/90/0/(\mp 45)_2$
2	$(\pm 45)_2/0/90/(\pm 45)/0/[0_6]/0/(\mp 45)/90/0/[0_5]/(\mp 45)_2$
3	$(\pm 45)_2/0/[0_6]/90/(\pm 45)/0_2/(\mp 45)/90/0/[0_5]/(\mp 45)_2$
4	$(\pm 45)/0/(\pm 45)/[0_6]/90/0/(\pm 45)/(\mp 45)/0/[0_5]/90/(\mp 45)/0/(\mp 45)$
5	$(\pm 45)/0/(\pm 45)/90/0/(\pm 45)/(\mp 45)/0/90/(\mp 45)/0/(\mp 45)/[(\pm 45)/0_3/90/0_3/(\mp 45)]$
6	$(\pm 45)_2/0/[0_6]/B/90/(\pm 45)/0/[0_5]/0/(\mp 45)/B/90/0/(\mp 45)_2$

note: B = bond film; plies between [ ] are doubler plies

### 3. EXPERIMENTAL PROCEDURE

Low velocity impact damage was applied to the first three specimens of each lay-up with an instrumented impactor, at the flat skin opposite to the edge of the doubler as shown in Fig. 4. The impactor used had a mass of 2.312 kg and a semi-spherical tup with a diameter of 1.0 inch (25.4 mm). The impact energy was 35J for the first specimen and 50J for the second and third specimens of each lay-up. The fourth specimen of each lay-up was statically indented up to the same deflection as the maximum deflection measured during the 35J impacts. The fifth specimen of each lay-up was left undamaged. All damaged specimens were C-scanned, and the first specimen of each lay-up was dissected for a post-mortem investigation of the impact damage.

After impact damage was induced, the specimens were loaded in static uni-axial compression up to failure (or up to a compressive strain of 0.0070 in case of several of the undamaged specimens), mounted in the anti-buckling guide shown in Fig. 5. Displacements were measured with LVDT's, and strains with strain gauges at locations also shown in Fig. 5. The failure mode was established with post-mortem fractography for specimens '3' of each lay-up.

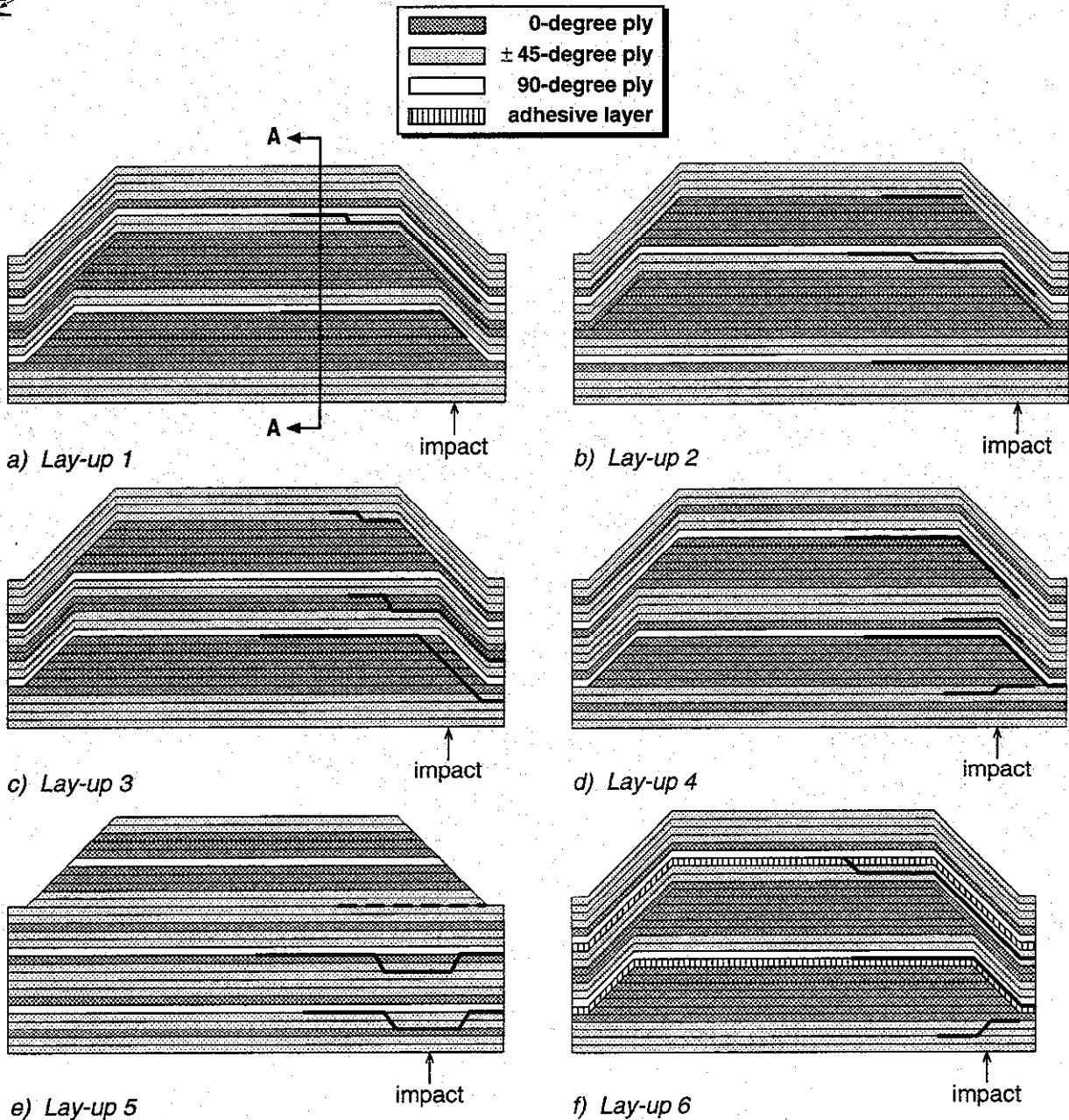


Fig. 4 Lay-ups of six SR-specimens with major impact induced delaminations (cross-section A - A refers to figure 8)

## 4. RESULTS AND DISCUSSION

### Impact damage

Impact parameters are not discussed, except to indicate that the static and dynamic (35J) responses of the SR specimens were very close, as shown in Fig. 6 for Lay-up 1. This similarity may warrant the approach to design for "static" rather than dynamic impacts, an observation which may simplify optimization procedures in the future, as static responses are easier to compute. The first specimen of each lay-up was dissected, and the major delaminations were made visible with uv-light, illuminating a penetrating fluid (Fig. 7). The cross sections shown are located at a distance of approximately 20 mm from the impact site to eliminate the smaller delaminations. The location of the major delaminations relative to the stacking sequence are indicated in Fig. 4 for all six lay-ups.

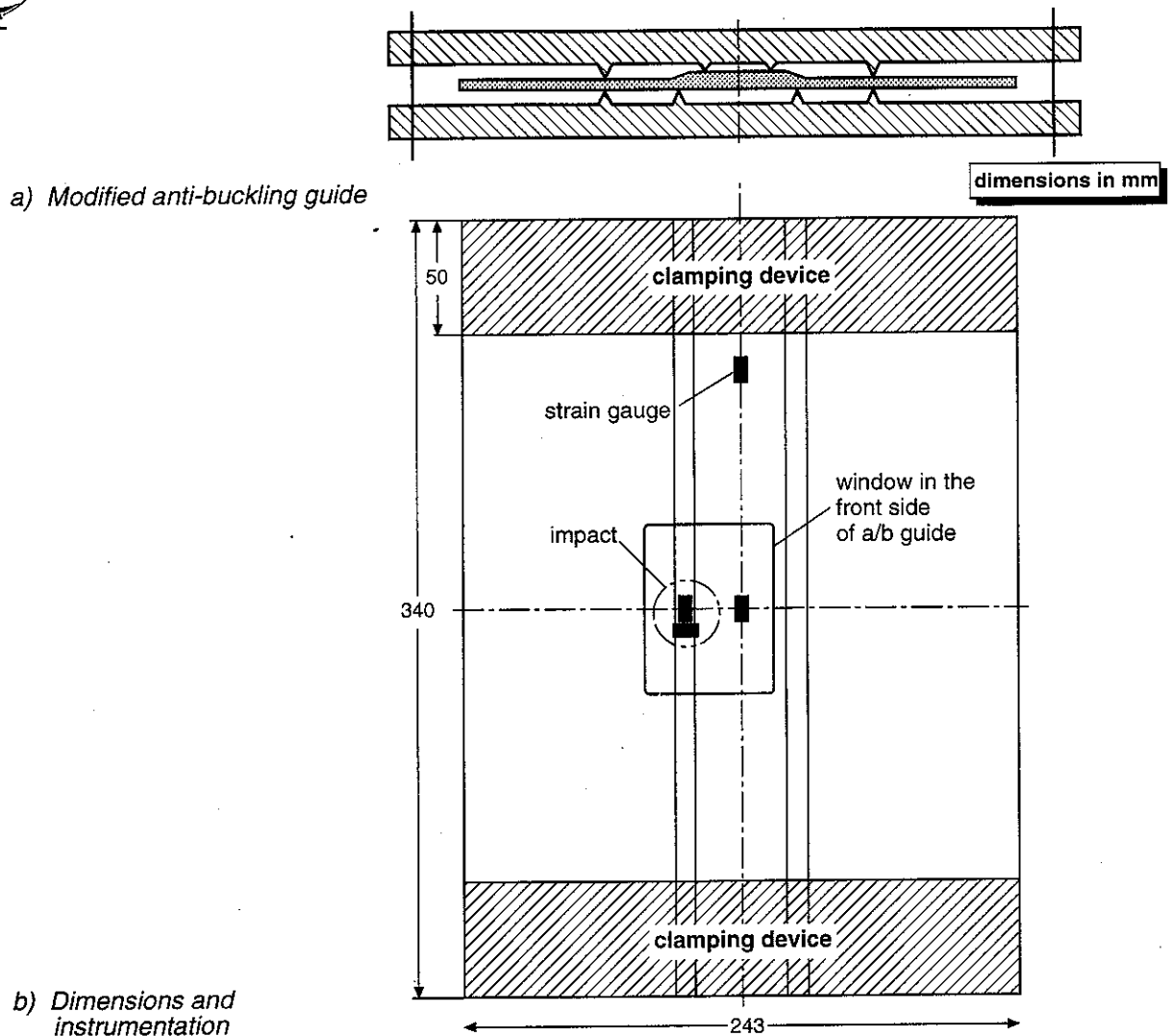


Fig. 5 Test configuration of SR-specimens

In the following discussion the damage is described with reference to the impact direction: the front is the flat, impacted side of the laminate. Most lay-ups contained two 0-degree ply stacks and all lay-ups contained two 90-degree skin plies. The major impact induced delaminations were expected to occur behind the 0-degree ply stacks and along the 90-degree plies when these were nearby. Lay-up 1 shows two major delaminations behind the two 0-degree ply stacks, and along or close to the 90-degree plies which are located behind these ply stacks, as expected. Lay-up 2 shows three major delaminations: two behind the 0-degree ply stacks, very deep inside the laminate, but also one in front of the first ply stack, very close to the free surface. This undesirable delamination is caused by the presence of a 0/90 degree ply interface in front of the first ply stack. Lay-up 3 also shows two major delaminations behind the 0-degree ply stacks. However, another large delamination is found in the wide space between the two thick 0-degree ply stacks, behind a thinner stack of two 0-degree skin plies that pass through this space. Lay-up 4 shows two large delaminations behind the two doubler ply stacks, as well as two smaller delaminations in front of each doubler ply stack. The two continuous 0-degree skin plies passing in front of the two doubler ply stacks are apparently responsible for these smaller delaminations. Lay-up 5 has a discrete doubler ply stack located on top of an uninterrupted flat skin. The damage, very different in character compared to the damage of the other lay-ups, resembles damage in a quasi-isotropic flat laminate, where the many ply angle changes (stiffness jumps) result in a larger number of smaller delaminations. The widest ones are located along the two 90-degree plies. Lay-up 6 is identical with Lay-up 1, except for two bond



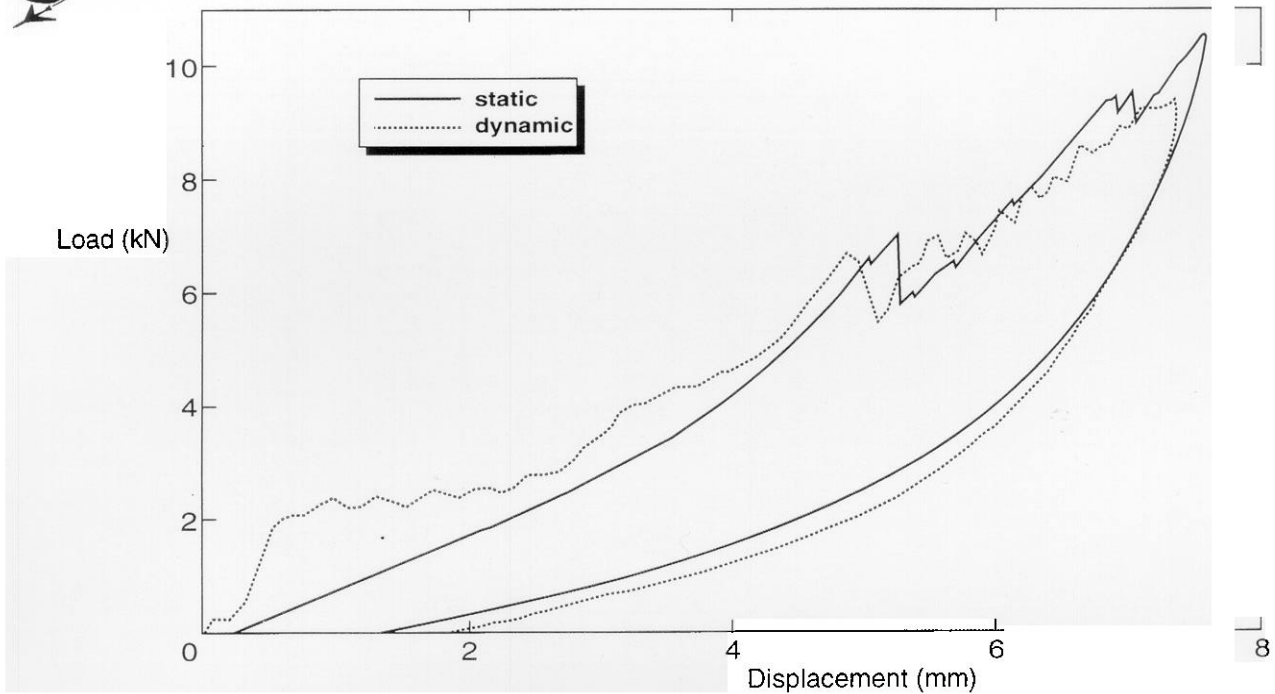
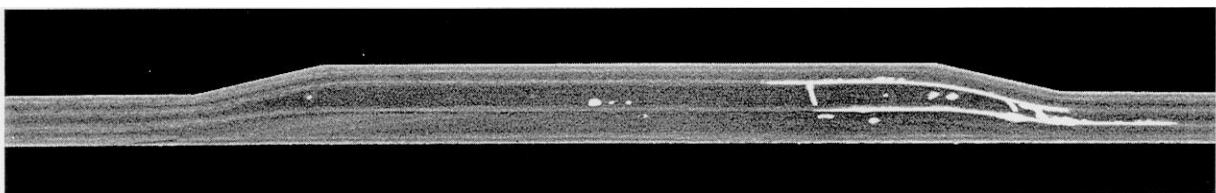


Fig. 6 Dynamic response (35 J) versus static response for lay-up 1

films added immediately in front of the two 90-degree plies. Just as for Lay-up 1, the major delaminations are located behind the doubler ply stacks. The bond layers apparently had no benevolent effect on the size of the impact damage.

Ranking the six lay-ups for expected "damage tolerance", based on the location and size of the major impact induced delaminations, and in correspondence with the postulated failure mechanism of buckling sublaminates, the following order (from best to worst) was tentatively established: Lay-ups 1, 6, 3, 2, 4 and 5. Apparently, to "place" delaminations deep inside a laminate, and to avoid the formation of additional undesirable delaminations at other locations, the number of ply angle changes should be limited. This can best be achieved by stacking the 0-degree doubler stacks adjacent to the 0-degree plies of the skin, by positioning the 90-degree plies immediately behind the 0-degree ply stacks where they will certainly provoke the formation of the major delaminations, and by surrounding these "planks" with uninterrupted  $\pm 45$  ply stacks.



a) Lay-up 1



b) Lay-up 3

Fig. 7 Major delaminations in SR specimens



Failure mechanisms

Specimens 2-5 of each lay-up were loaded in compression up to failure, or up to a compressive strain of 0.0070 for some of the undamaged specimens (to prevent damage to the test instrumentation). The maximum loads achieved are shown in table 2. The size of the total C-scan damage area is also presented for these specimens. Most configurations had C-scan areas of approximately 1800 mm<sup>2</sup>. The C-scan areas for Lay-up 4 are somewhat smaller at 1500 mm<sup>2</sup>, and the C-scan areas of Lay-up 5 (with a discrete doubler on top) are showing a much larger scatter, from 1450 mm<sup>2</sup> to 2450 mm<sup>2</sup>. This scatter is related to the large delamination occurring between doubler and skin, which is less consistent than the "enclosed" delaminations of the other configurations.

It appears from table 2 that the maximum loads of the undamaged specimens (specimens 5 of each lay-up) are much higher than those of the damaged specimens, all corresponding to axial compressive strains in excess of 0.0070. It should be noted that the axial stiffness of Lay-up 5 is less than the stiffness of the other lay-ups, because its discrete doubler stack on top of the skin is "softer" than  $O_{11}$  (to limit the stiffness difference between soft skin and stiff doubler). The failure loads of indented specimens 4 are, like the damage areas, of the same order of magnitude as those of the impacted specimens 2-3. For five of the six lay-ups the failure loads of the damaged specimens were very close. For Lay-up 4 the difference between specimens 2 and 3 was much larger (20%). This difference is due to the different failure modes observed for these two specimens: bending of the damaged area toward the window in the anti-buckling frame support (Fig. 5), or bending backward against the support. It must be concluded that the SR specimens do not provide residual strength values representative of the stiffened panel configuration. Unlike for the thicker (and stiffer) SR specimens described in [1-2], the absence of the stiffener can not be fully compensated by the influence of the support, which can push but not pull. Hence, the final failure mode of most specimens was by buckling in the direction away from the support into the window. Two of the higher failure values were observed for specimens which bent in the opposite direction, toward the support (specimens 2 of Lay-up 3 and Lay-up 4).

Table 2: Damage areas and failure loads

Config-uration	Specimen number	C-scan area (mm <sup>2</sup> )	Failure load (kN)	Config-uration	Specimen number	C-scan area (mm <sup>2</sup> )	Failure load (kN)
1	1	1610	-	4	1	1450	-
	2	1810	236		2	1558	275
	3	1877	229		3	1665	219
	4	1638	255		4	1346	238
	5	-	362		5	-	294*
2	1	1530	-	5	1	1570	-
	2	1874	229		2	1445	203
	3	1699	230		3	1916	222
	4	1867	234		4	2451	232
	5	-	372		5	-	270*
3	1	1600	-	6	1	1650	-
	2	1764	249		2	1827	266
	3	1963	259		3	1634	266
	4	1698	246		4	1700	264
	5	-	295*		5	-	306*

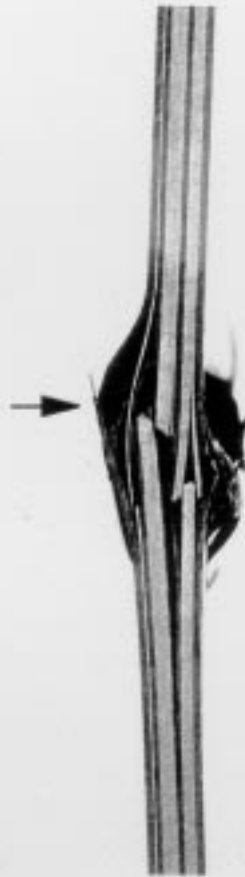
\* (test stopped at a compressive strain of 0.0070)

flat side

impact location



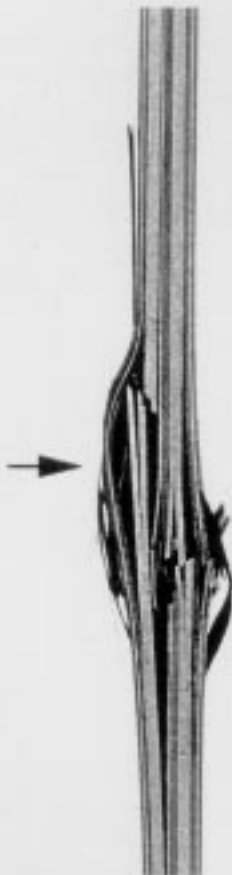
a) Lay-up 1



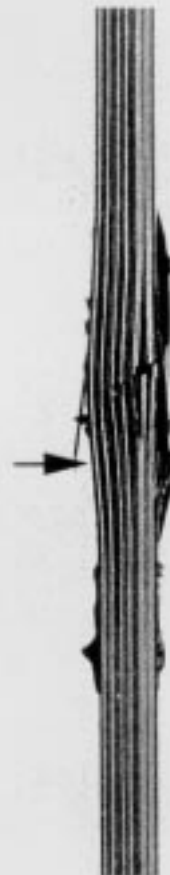
b) Lay-up 2



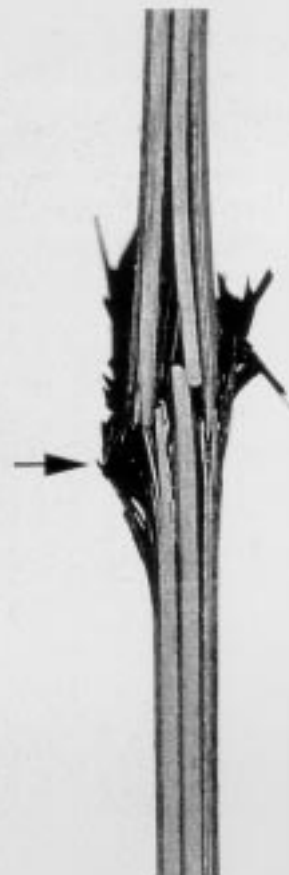
c) Lay-up 3



d) Lay-up 4



e) Lay-up 5



f) Lay-up 6

Fig. 8 Post-mortem cross-sections of SR specimens "3", as indicated in figure 4a (A-A)



However, to validate the postulated failure mechanism, of major delaminations growing and sublaminate buckling, post-mortem cross sections (as indicated by A-A in Fig. 4a) were made of specimens 3 of each lay-up, all of which had failed in the same mode: buckling away from the support (opposite to the impact direction). Photographs of these sections are shown in Fig. 8 of the skin/doubler zone, in which the 0-degree plies are visible as the lighter layers. The failure loads of these specimens were 259/266J for Lay-ups 3 and 6, 229/230 J for Lay-ups 1 and 2, and 219/222 J for Lay-ups 4 and 5. Comparing this order of "damage tolerance" to the order concluded above on the basis of the impact induced delaminations, there is not much difference: Lay-up 3 was better than expected and changed positions with Lay-up 1, most likely because it is an almost symmetric laminate and remained straight up to higher loads. Lay-up 6, thought to be equivalent to Lay-up 1 because it has the same stacking sequence, while the added bond layers had not limited the size of the damage, was actually better than Lay-up 1. The superior residual strength of Lay-up 6 may be caused by a higher resistance against delamination spread or by the improved stability due to the added thickness of the bond layers. Based on the post-mortem results it is concluded that the postulated failure mechanism is correct in the sense that the major impact induced delaminations located behind the 0-degree doubler plies are the delaminations that grow, driven by the buckling or bending of these ply stacks. However, the differences between the failure loads of the different lay-ups are smaller than expected, indicating that buckling of the delaminated sublaminates is not the only acting failure mechanism. From the photographs in Fig. 8 it is clear that ultimate failure occurs by transverse shear of the unsupported 0-degree ply stacks. This failure mechanism does not seem to depend much on the location of the 0-degree ply stacks, but rather on the amount of transverse shear deformation that occurred. Increasing the global stability of the laminate, by maintaining symmetry even in the doubler area (Lay-up 3) or by increasing the laminate thickness with bond layers (Lay-up 6) apparently resulted in a higher damage tolerance. The global stability of an impacted laminate is also increased by the presence of a stiffener. In fact, stiffened panels, made according to the same design as shown in Fig. 2, and tested in compression with similar impact damage [3], failed at much higher strains of 0.0062 and 0.0070 than the 0.0050-0.0055 observed for the damaged SR specimens. The failure modes of the panels were not even related to these damages, which illustrates the effect of the support of stiffeners in particular, and the damage tolerance of Boeing's design concept in general.

## 5. CONCLUDING REMARKS

Impact damage and failure mechanisms were studied using small (unstiffened) structure relevant (SR) specimens. By varying the stacking sequence of the skin/doubler laminate it was tried to influence the location of the major impact induced delaminations within the laminate. It was believed that delaminations located deeper inside a laminate would lead to improved damage tolerance. Results for six different lay-ups were compared, and the major delaminations were found at the ply interfaces where they were expected. In some cases, additional "undesirable" delaminations were found also.

Subsequently, damaged and undamaged specimens for each lay-up were loaded in compression while supported in an anti-buckling frame; the damage reduced the residual strength as expected. For five of the six lay-ups the failure loads of the damaged specimens were very close. The failure loads for the damaged specimens of the sixth lay-up were 20% apart due to the occurrence of different failure modes. Specimens which were damaged by slow indentation showed similar damage and similar residual strength as impact damaged specimens. This may have important implications for design optimization procedures, as static responses are easier to compute than dynamic responses.

A postulated failure mechanism was confirmed to a certain extent, in the sense that the major impact induced delaminations were indeed the delaminations that propagated, driven by the



bending or buckling of the doubler ply stacks. However, transverse shear of the increasingly unsupported 0-degree ply stacks became the ultimate failure mechanism. As a result of these observations, it will be undertaken to develop a failure criterion based upon the interaction of longitudinal compressive strain  $\epsilon_x$  and transverse shear strain  $\gamma_{xz}$  for 0-degree dominated ply stacks.

## 6. ACKNOWLEDGEMENTS

The work on damage tolerance of composite structures described in this paper is part of a wider research programme carried out at NLR. This particular task was carried out for the Netherlands Agency for Aerospace Programs (NIVR).

## 7. REFERENCES

1. Labonté, S. and Wiggenraad, J.F.M., "Development of a Structure Relevant Specimen for Damage Tolerance Studies", presented at the 9th International Conference on Composite Materials (ICCM-9), Madrid, Spain, 12-16 July 1993.
2. Labonté, S. and Wiggenraad, J.F.M., "A Damage Tolerance Study Conducted with Structure Relevant Specimens", NLR TP 93067 U, 1993.
3. Ubels, L.C. and Wiggenraad, J.F.M., "A Method to Apply Structure Relevant Impact Damage to Small Structure Relevant Specimens for Damage Tolerance Studies", presented at the 10th International Conference on Composite Materials (ICCM-10), Whistler, Canada, 14-18 August, 1995.
4. McCarty, J.E. and Roeseler, W.G., "Durability and Damage Tolerance of Large Composite Primary Aircraft Structure", NASA CR-003767, 1984.
5. Arendsen, P., Thuis, H.G.S.J. and Wiggenraad, J.F.M., "Optimization of Composite Stiffened Panels with Postbuckling Constraints", 4th CADCOMP, Southampton, UK, 1994.